

Effect of Alloy Elements in Time Temperature Transformation Diagrams of Railway Wheels

A.B. Rezende¹, F.M Fernandes¹, S.T. Fonseca¹, P.F.S. Farina¹,
H. Goldenstein² and P.R. Mei^{1,a}

¹State University of Campinas, Faculty of Mechanical Engineering, 13083-860, Campinas, Brazil.

²University of São Paulo, Metallurgical and Materials Engineering Department, 05508-030, São Paulo, SP, Brazil

^apmei@fem.unicamp.br

Keywords: microalloyed steel, TTT diagrams, niobium, vanadium, railway wheels, bainite.

Abstract: The Heavy-Haul railroad wheels started to use higher wear resistance steels microalloyed with niobium, vanadium, and molybdenum [1]. During continuous cooling, these elements depress the temperature of the pearlite formation, producing smaller interlamellar spacing that increases the hardness of the steel, besides to favor the precipitation hardening through the formation of carbides [2, 3]. Also, they delay the formation of diffusional components like pearlite and bainite during isothermal transformation. The effects of these alloy elements on microstructure during isothermal transformation were studied in this work using a Bähr 805A/D dilatometer. Three different compositions of class C railway wheels steels (two microalloyed and one, non microalloyed) were analyzed in temperatures between 200 and 700 °C. The microstructure and hardness for each isothermal treatment were obtained after the experiments. Comparing with non microalloyed steel (7C), the vanadium addition (7V steel) did not affect the beginning of diffusion-controlled reactions (pearlite and bainite), but delayed the end of these reactions, and showed separated bays for pearlite and bainite. The Nb + Mo addition delayed the beginning and the ending of pearlite and bainite formation and also showed distinct bays for them. The delays in diffusion-controlled reactions were more intense in the 7NbMo steel than in 7V steel. The V or Nb + Mo additions decreased the start temperature for martensite formation and increased the start temperature for austenite formation.

Introduction

The research for materials that present better mechanical properties for railway wheels has been the focus of the industries in the last years. The pearlite microstructures have been widely used in railway wheels and rails over the years and did not undergo significant changes since the beginning of its use. Recent researches have sought to reduce the interlamellar spacing and the colonies size of the pearlite using microalloyed steels and combination of thermal and thermomechanical treatments routes [4]. Microalloyed steels are manganese-carbon steels containing small amounts (less than 0.1% in mass) of strong carbide-forming elements such as niobium, vanadium, molybdenum, and titanium. These elements in solid solution, during continuous cooling, depress the temperature formation of pearlite, producing smaller interlamellar spacing that increases the hardness. The fine carbides precipitated also prevent the growth of the austenitic grain during the cooling, contributing to the increase of the toughness. When added together with the niobium, molybdenum increases the number of Nb(C,N) particles and they are finer, which increases the potential for the precipitation hardening [5]. The addition of these elements proved to be promising in reducing wear on railway wheels [6]. However, the increase in mechanical strength from pearlitic microstructures has reached the limit, which makes it necessary to search for alternative microstructures for application on wheels and rails [7]. In the last years, researchers have developed steels with bainitic microstructure for wheels and rails that present higher values of mechanical resistance, toughness and wear resistance than those provided by the pearlite microstructure [8-10]. The microconstituents (pearlite, ferrite, and cementite) occur from the austenitic field when the material is subjected to slow cooling, but when the cooling is faster other metastable constituents may appear, such as bainite and martensite. To follow the formation of these

constituents are used TTT curves (temperature, time, and transformation), which can predict the temperatures and times for the establishment of each microconstituent. Thus, in this work, we study the effect of the addition of vanadium, niobium, and molybdenum on the isothermal transformation curves (ITT) of a class C steel of the AAR standard used in railway wheels.

Materials and Methods

The specimens were taken from three forged railway wheels with different chemical compositions (Table 1). As a reference, a Class C wheel (carbon steel) was used. In the second wheel were added niobium and molybdenum (7NbMo steel) and in the third wheel was added vanadium (7V steel).

Table 1 - Chemical composition of the steels used in this work (weight %)

Steel	C	Si	Mn	P	S	Mo	Nb	V
7C	0.74	0.30	0.79	0.018	0.009	-	-	-
7NbMo	0.71	0.43	0.84	0.017	0.008	0.203	0.02	-
7V	0.68	0.55	0.88	0.007	0.011	-	-	0.13

The isothermal transformation curves were obtained by dilatometry tests performed on Type 805 A/D dilatometer, available at the USP / SP - Phase Transformation Laboratory. The CPs used had a cylindrical shape with a diameter of 4 mm and a length of 10 mm. The procedure to obtain the isothermal cooling curve consisted of austenitizing the material at 880 °C for 5 min, followed by abrupt cooling (rate of 20 °C/s) up to the isothermal transformation temperature, maintaining at this temperature for the time necessary to the transformation of the phases and subsequent slow cooling to room temperature. The following temperatures were used for isothermal transformation: 700, 650, 600, 550, 500, 450, 400, 350, 300, 250 and 200°C.

A scanning electron microscope (SEM) from Unicamp, model Zeiss EVO MA 15 was used. The hardness was measured using a Future Tech durometer, model FV with a load of 0.5 kgf applied during 15 seconds. A "Panalitical X'pert Pro" diffractometer of the CNPEM / LNNano was used for X-ray diffraction, with the parameters: Co K α radiation, 40 kV, 45 mA, angle 2 θ from 40° to 130°.

Results and Discussion

Dilatometric results and microstructure for samples treated at 700, 650, 300 e 200 °C are showed in Figures 1 to 4. At 700 °C the pearlitic reaction for 7NbMo was not completed up to 30 minutes, and the microstructure presented pearlite and also martensite and retained austenite after cooling to room temperature, as can be seen in Fig. 3. Fast cooling (20 °C/s) from 880 °C (fully austenitic) to 200 °C promoted the partial formation of martensite, since this temperature is below the start temperature for martensitic formation (Ms). The permanence of samples of all steels (7V, 7C, and 7NbMo) at 200 °C promotes reactions detected by the dilatometer. These reactions can be the precipitation of carbides from retained austenite, the formation of fresh martensite due the decreasing of the carbon level in the austenite, the tempering of the previous martensite formed, the formation of lower bainite, or the simultaneous occurrence of several reactions. X-ray diffraction (Fig. 5) confirmed the martensite formation and retained austenite, but it is not possible to assure that there was also bainite formation with XRD, because the peaks of bainite and martensite presented superimposed (Table 2). Silva et al. [11] observed in 0.3C-3Mn-1.5Si steel the formation of lower bainite and tempered martensite after austenitizing and fast cooling (20 °C/s) to temperatures below the martensite starting temperature, and holding isothermally the samples for one hour.

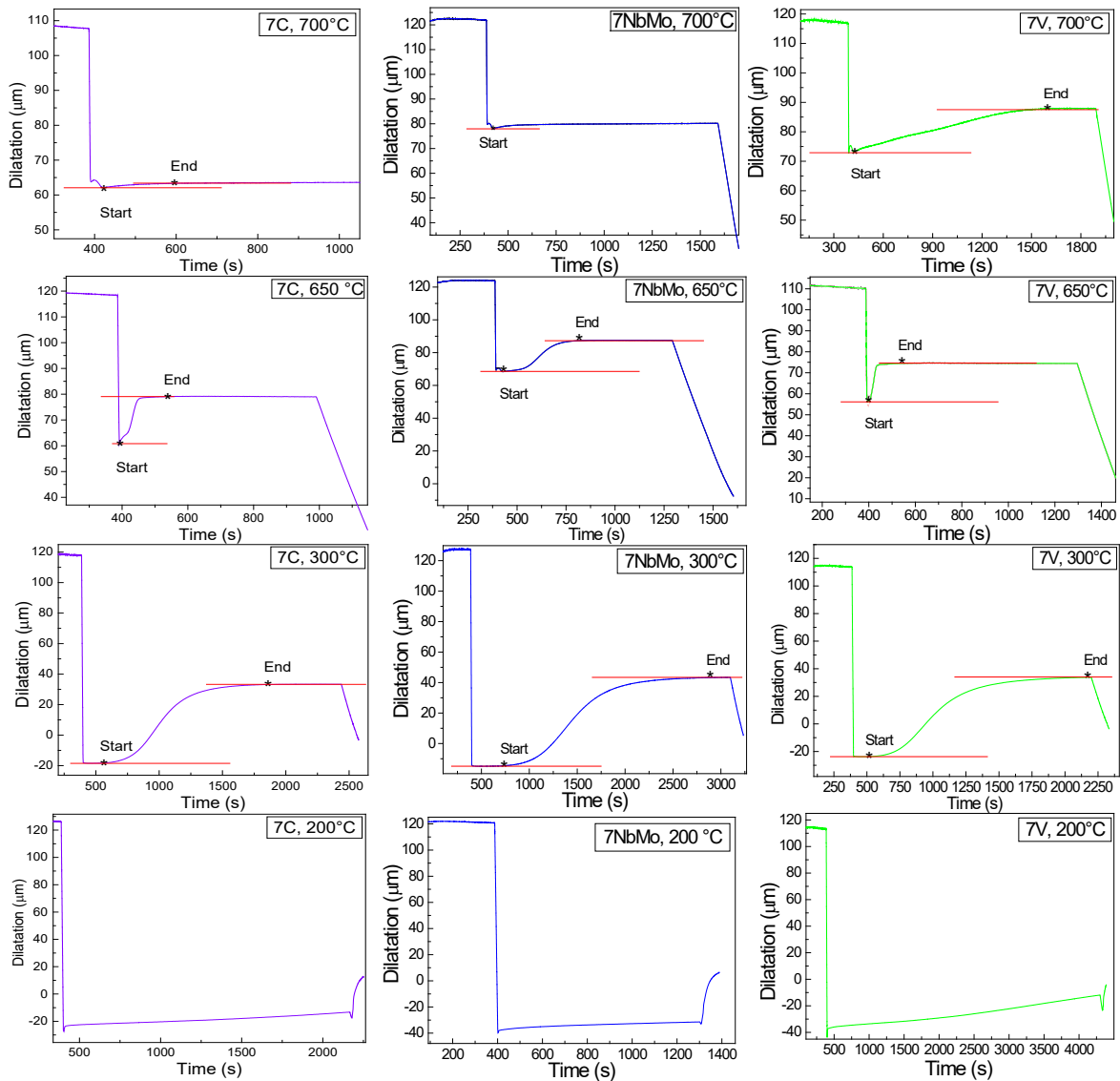


Figure 1 – Dilatometric curves for 7C, 7V and 7NbMo steels with isothermal treatment at 700, 650, 300 and 200°C.

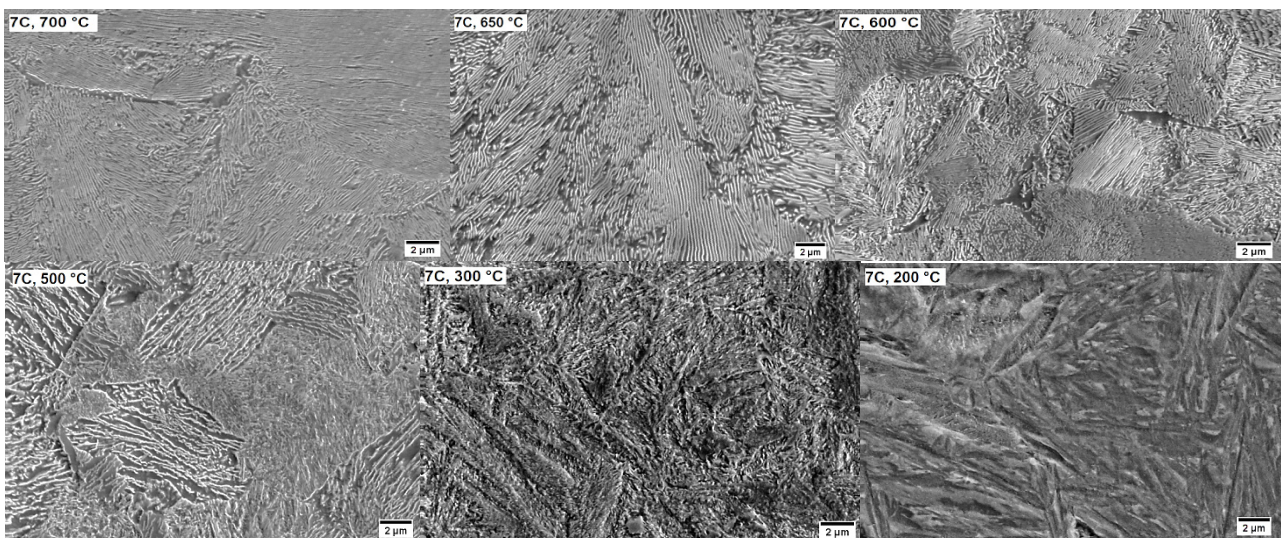


Figure 2 – Microstructures obtained for 7C steel after isothermal treatment at 700, 650, 600, 500, 300 and 200°C, Nital 2%.

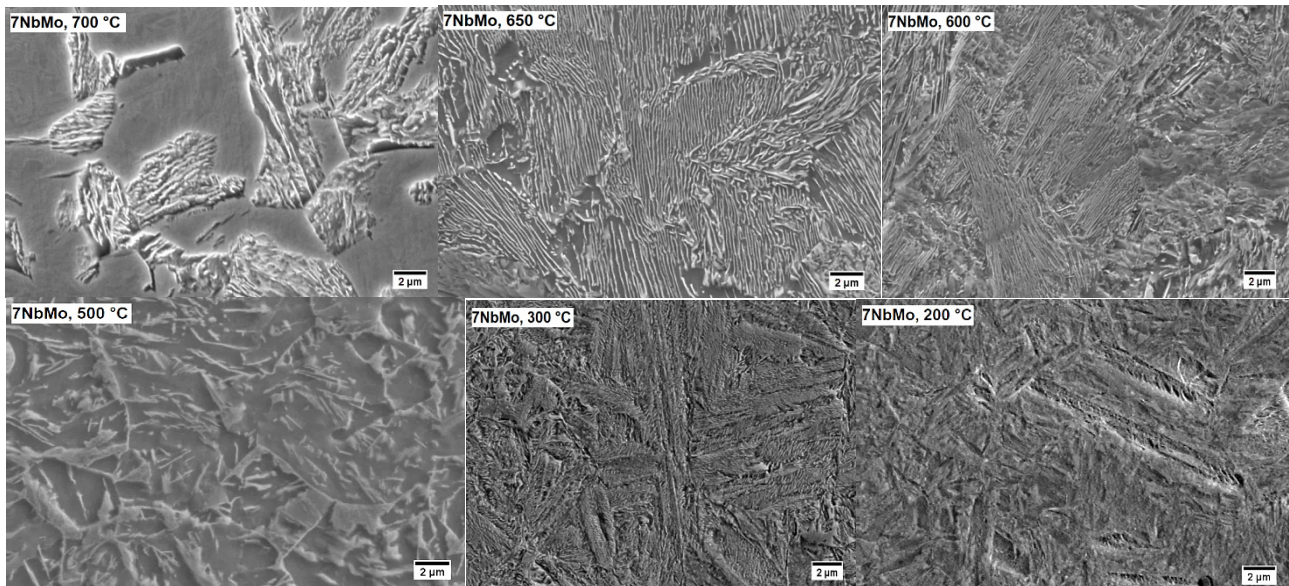


Figure 3 – Microstructures obtained for 7NbMo steel after isothermal treatment at 700, 650, 600, 500, 300 and 200 °C. Nital 2%.

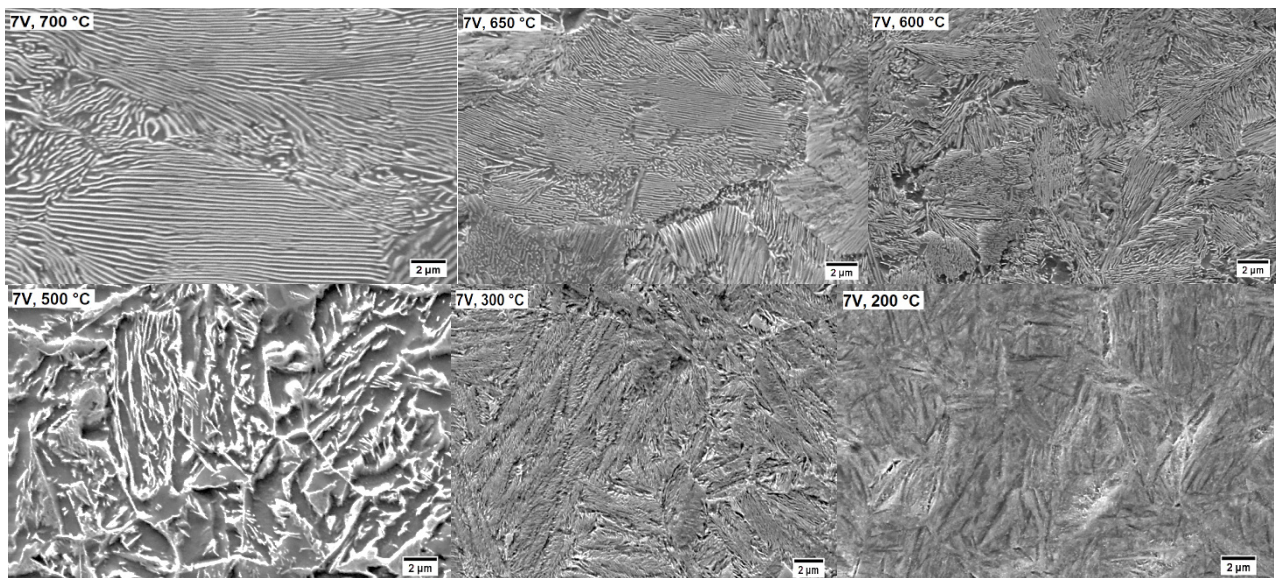


Figure 4 – Microstructures obtained for 7V steel after isothermal treatment at 700, 650, 600, 500, 300 and 200 °C. Nital 2%.

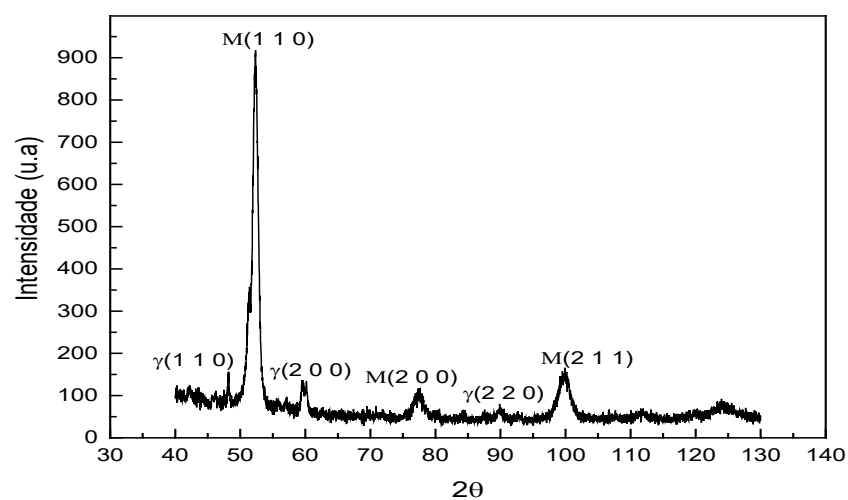
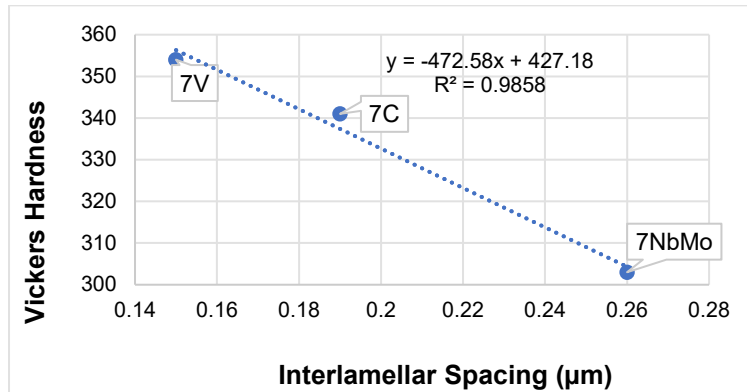


Figure 5 - X-ray diffraction for 7NbMo steel after isothermal treatment at 200 °C.

Table 2 – X-ray diffraction peaks for bainite and martensite using cobalt tube ([12][13]).

Planes	Bainite 2θ	Martensite 2θ
(110)	52.9	53.9
(200)	77.7	76.3
(211)	96.8	99.0

**Figure 6** – Linear correlation between the interlamellar spacing of pearlite and Vickers hardness for 7C, 7C and 7NbMo steels after isothermal treatment at 650 °C.**Table 3** – Pearlite interlamellar spacing, Vickers hardness and austenitic grain size after isothermal treatment at 650 °C.

Steel	7C	7NbMo	7V
Interlamellar Spacing (µm)	0.19 ± 0.02	0.26 ± 0.03	0.15 ± 0.02
Vickers Hardness (HV)	333 ± 2	303 ± 12	354 ± 4
Austenitic Grain Size (µm)	12 ± 1	8 ± 1	6 ± 1

The 7V and 7NbMo steels presented smaller AGS (Austenitic Grain Size) than 7C steel (6; 8 and 12 µm, respectively), due to the precipitation of fine V, Nb, Mo carbonitrides during the forging process, which pinning the austenitic grain boundary and difficult its growth (Table 3). After 650 °C isothermal transformation, the 7V steel presented the smallest PIS (Pearlite Interlamellar Spacing): 0.15; 0.19 and 0.26 µm for 7V, 7C, and 7NbMo, respectively, showing that the AGS does not determine the PIS directly, but also depends on others effects of the microalloying elements on the Fe-C diagram. But, on the other hand, the Vickers hardness on these steels showed a linear dependence of PIS [HV = 427 – 473.PIS (in µm)] as can be seen in Fig. 6.

To determine the martensite start temperature (Ms), the samples were cooled from austenitizing temperature (880 °C) at high speed (20 °C/s), as showed in Fig. 7, and the results are in Table 4. The V or NbMo addition decreased the start temperature for martensite formation (Ms = 214, 210, and 221 °C for 7V, 7NbMo and 7C, respectively). Carbon, manganese and silicon additions reduce the Ms and, as the steels used had different amounts of these elements, some empirical equations from the literature were used to predict the specific effect of these elements on the Ms (Table 5). The Ms should be lower in the 7C steel compared to 7V and 7NbMo steels, regarding only to effect of C, Mn, and Si. But the real measurements showed the opposite, meaning that V or NbMo additions caused a reduction on the Ms in these steels.

Carbon, manganese and silicon additions also affect A1 temperature and, as the steels used had different amount of these elements, using Trzaska [14] equation [Ac1 = 472 – 29 C – 14 Mn + 13 Si] to predict the effect of these elements, we obtain 713, 715 and 717 °C for 7C, 7NbMo and 7V steels, respectively, or near the Ac1 for the three steels. Meanwhile, the V or NbMo addition increased significantly the start temperature for austenite formation (741, 754 and 760 °C, for 7C, 7NbMo, and 7V steels, respectively), which was expected, since these elements have bcc structures and are ferrite stabilizers, contracting the austenitic field. For the other, the contracting of the austenitic field brought more closely the end temperature for austenite formation (768, 772 and 775 °C, for 7C, 7NbMo, and 7V steels, respectively).

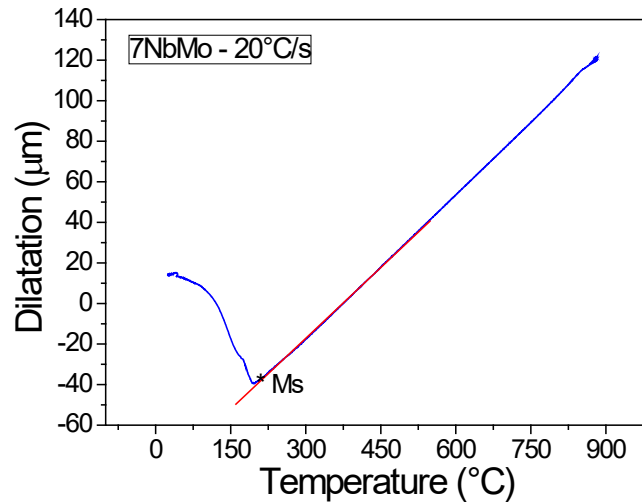


Figure 7 - Determination of Ms (Martensite Start temperature) with fast cooling (20 °C/s) from austenitizing temperature (880 °C) using 7NbMo steel.

Table 4 – Austenite and martensite transformation temperatures for 7C, 7NbMo, and 7V steels.

Steel	7C	7NbMo	7V
Austenite Start (°C)	741	754	760
Austenite End (°C)	768	772	775
Martensite Start (°C)	221	210	214

Table 5 - Expected Martensite Start temperature (Ms) related only to C, Mn, and Si and the real Ms

Steel	[14]Trzaska (°C)	[15]Capdevila (°C)	[16]Kunitake (°C)	Calculated Mean* (°C)	Real (°C)
7C	213	238	226	226	221
7NbMo	221	244	236	234	210
7V	231	250	246	242	214

Ms = 491 – 302.6C – 30.6Mn -14.5Si (Capdevila); Ms = 560 – 407.3C – 37.8Mn -7.3 Si (Kunitake); Ms = 541 - 401C -36 Mn -10,5Si (Trzaska); Calculated Mean* = [Ms (Capdevila) + Ms (Trzaska) + Ms (Kunitake)]/3

Vickers hardness for 7C, 7NbMo e 7V steels samples after isothermal treatment (Fig. 8) showed that, as the temperature decreased from 650 °C to 600 °C, the hardness increased in all steels due to the pearlite refinement, since there was no great difference in free ferrite fraction (Table 6). However, during the transition from pearlite to upper bainite, there was a decreasing of hardness in all steels, reaching a minimum value at 500 °C and with a structure that looks like granular bainite in 7V and 7NbMo steels. Below this temperature, the lower bainite increased its volume fraction, and the hardness increased continuously as the temperature decreased.

Comparing with non microalloyed steel (7C), the vanadium addition (7V steel) did not affect the beginning of diffusion-controlled reactions (pearlite and bainite), but delayed the end of these reactions, and showed separated bays for pearlite and bainite (Fig. 9). The Nb+Mo addition delayed both, beginning and ending of pearlite and bainite formation and showed distinct bays for pearlite and bainite. The delays in diffusion-controlled reactions were more intense in the 7NbMo steel than in 7V steel.

Medium and high carbon steels, with or without vanadium or niobium microadditions, with pearlitic/bainitic microstructures have been studied by various research groups in recent years [17-36]. The results are used to produce more wear-resistant wheels and rails, extending the life of these components and reducing the cost of the railroad transportation. The results obtained in this work contribute to this development.

Table 6 - Vickers hardness (HV), pearlite interlamellar spacing (PIS) and free ferrite at temperatures that present lamellar structure (600 and 650°C).

Temperature (°C)	7C			7V			7NbMo		
	HV	PIS (µm)	Ferrite (%)	HV	PIS (µm)	Ferrite (%)	HV	PIS (µm)	Ferrite (%)
650	341	0.19	1.0%	354	0.15	1.9%	303	0.26	1.2%
600	361	0.14	0.9%	392	0.11	1.5%	334	0.20	1.5%

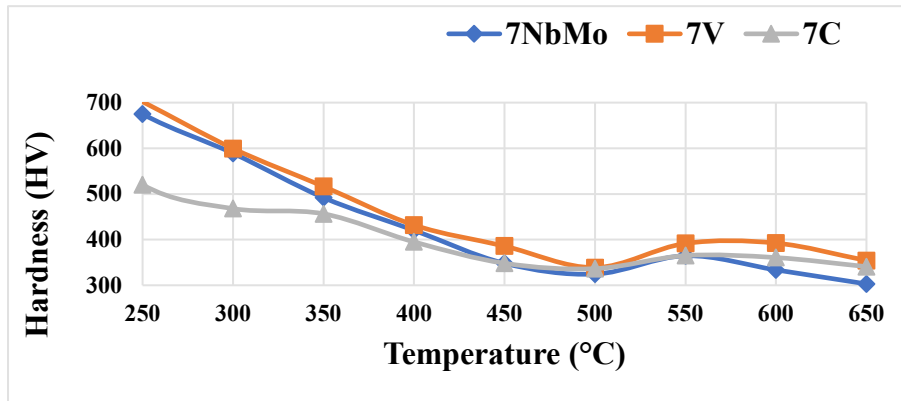


Figure 8 - Vickers hardness for 7C, 7NbMo e 7V steels samples after isothermal treatment.

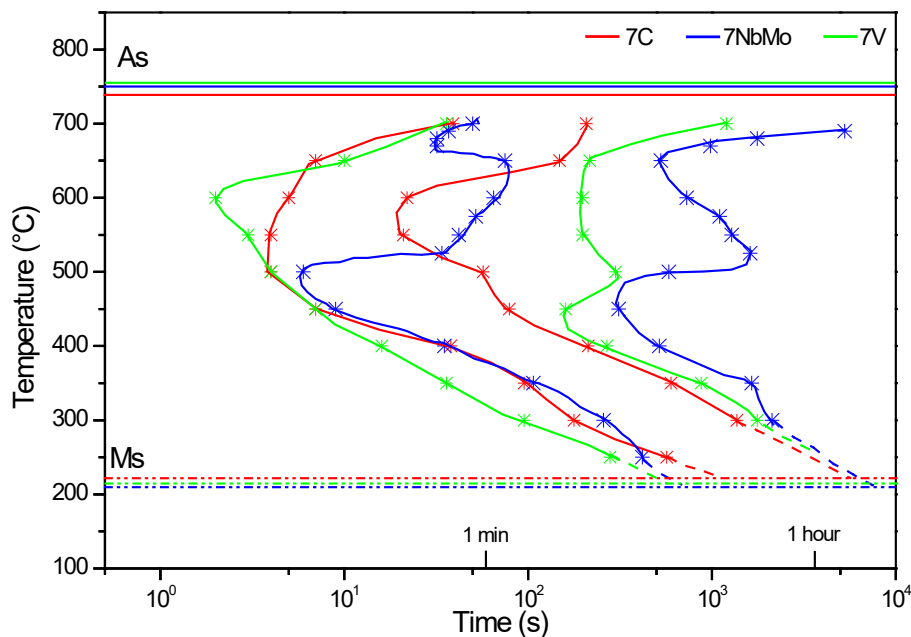


Figure 9 – Isothermal transformation (ITT) diagrams for 7C, 7NbMo e 7V steels.

Conclusions

Three railway wheels using steels with the basic composition 0.7C/0.8 Mn/0.4 Si were produced by forging process. One, without microalloying addition (7C); the second, microalloyed with 0.13V (7V) and the third, with 0.2Mo + 0.02Nb addition (7NbMo). After austenitizing at 880 °C and isothermal transformation in the range 700- 200 °C, the following conclusions were obtained:

1. The permanence of samples of all steels at 200 °C (below Ms), after austenitizing and fast quenching, promoted diffusion-controlled reactions detected by the dilatometer.
2. The 7V and 7NbMo steels showed smaller AGS (Austenitic Grain Size) than 7C steel. After 650 °C isothermal transformation, the 7V steel presented the smallest PIS (Pearlite Interlamellar Spacing): 0.15; 0.19 and 0.26 µm for 7V, 7C, and 7NbMo, respectively, showing that the AGS does not determine the PIS directly.

3. Vickers hardness on these steels showed a linear dependence of PIS: [HV = 427 – 473.PIS (in μm)].
4. The V or NbMo additions decreased the start temperature for martensite formation and increased the start temperature for austenite formation.
5. As the temperature decreased from 650 °C to 600 °C, the hardness increased in all steels due to the pearlite refinement, since there was no great difference in free ferrite fraction. However, during the transition from pearlite to upper bainite, there was a decreasing of hardness in all steels, reaching a minimum value at 500 °C and with a structure that looks like granular bainite in 7V and 7NbMo steels. Below this temperature, the lower bainite increased its volume fraction, and the hardness increased continuously as the temperature decreased.
6. Comparing with nonmicroalloyed steel (7C), the vanadium addition (7V steel) did not affect the beginning of diffusion-controlled reactions (pearlite and bainite), but delayed the end of these reactions, and showed separated bays for pearlite and bainite. The NbMo addition delayed the beginning and the ending of pearlite and bainite formation and also showed distinct bays for them. The delays in diffusion-controlled reactions were more intense in the 7NbMo steel than in 7V steel.

Acknowledgments

The authors acknowledge the financial support provide by Vale S.A, CNPq (National Research Council) and Capes (Coordination for the Improvement of Higher Education). The research was supported by LNNano - Brazilian Nanotechnology National Laboratory, CNPEM/MCTIC - Metals Characterization and Processing Laboratory.

References

- [1] W. Yu, L. Liu, Y. Xia, C. Xi. The effect of vanadium on the phase transformation of the 82B steel, *J. Metall. Eng.*, 2 (2013) 140–148.
- [2] L. M. Panfilova, L. A. Smirnov. Bainitic refinement of machine steels microalloyed with vanadium and nitrogen, *Metallurgist*, 59, 11–12 (2016) 1062–1067.
- [3] Ě. Bohuslav, N. Miroslav, M. Petr. Residual stresses of railway wheels, in 50 th Annual Conference on Experimental Stress Analysis, (2012) 6.
- [4] C. Chattopadhyay, S. Sangal, K. Mondal, A. Garg. Improved wear resistance of medium carbon microalloyed bainitic steels, *Wear*, 289 (2012) 168–179.
- [5] R. Uemori, R. Chijiwa, H. Tamehiro, H. Morikawa. AP-FIM study on the effect of Mo addition on microstructure in Ti-Nb steel, *Appl. Surf. Sci.*, 76–77 (1994) 255–260.
- [6] A. B. Rezende, G. A. Amorim, D. J. Minicucci, S. T. Fonseca, P. R. Mei. Effect of vanadium addition on the surface roughness and fatigue crack propagation in a railroad wheel using twin disc wear test, *Defect Diffusion Forum*, 391 (2019) 66–73.
- [7] D. Zapata, J. Jaramillo, A. Toro. Rolling contact and adhesive wear of bainitic and pearlitic steels in low load regime, *Wear*, 271, 1–2 (2011) 393–399.
- [8] G. Girsch, R. Heyder. Advanced pearlitic and bainitic high strength rails promise to improve rolling contact fatigue resistance, in 7th World Congress on Railway Research (WCRR2006), 62, 1 (2006) 9.
- [9] P. Clayton, K. J. Sawley, P. J. Bolton, G. M. Pell. Wear behavior of bainitic steels, *Wear*, 120, 2 (1987) 199–220.
- [10] W. Solano-Alvarez, E. J. Pickering, H. K. D. H. Bhadeshia. Degradation of nanostructured bainitic steel under rolling contact fatigue, *Mater. Sci. Eng. A*, 617 (2014) 156–164.

-
- [11] E.P. Da Silva et al., Isothermal transformations in advanced high strength steels below martensite start temperature, *Mater. Sci. Technol.*, 31, 7 (2015) 808–816.
- [12] T. Takahashi, W. A. Bassett, M. Hokwang. Isothermal compression of the alloys of iron up to 300 kbar at room temperature. *J. Geophys. Res. B*, 73 (1968) 4717–4725.
- [13] R. Kohlhaas, P. Duenner, N. Schmitz-Pranghe. The temperature dependence of the lattice parameters of iron, cobalt and nickel in the range of high temperatures, *Zeitschrift fuer Angew. Phys.*, 23, 4 (1967) 245–249.
- [14] J. Trzaska. Calculation of critical temperatures by empirical formula, *Arch. Metall. Mater.*, 61 2B, (2016) 981–986.
- [15] C. Capdevila, F. G. Caballero, C. G. de Andrés. Determination of Ms temperature in steels: A Bayesian neural network model. *ISIJ Int.*, 42, 8, (2002) 894–902.
- [16] T. Kunitake. Prediction of Ac1, Ac3 and Ms temperatures by empirical formulas. *J. Japan Soc. Heat Treat.*, 41 (2001) 164–169.
- [17] M. Masoumi, E. A. A. Echeverri, A. Tschiptschin, H. Goldenstein. Improvement of wear resistance in a pearlitic rail steel via quenching and partitioning processing. *Nature: Scientific Reports*, 9, 7454 (2019) 01-12.
- [18] Z. Song, S. Zhao, T. Jiang et al. Effect of nanobainite content on the dry sliding wear behavior of an Al-alloyed high carbon steel with nanobainitic microstructure, *Materials*, 12 (10), 1618 (2019) 01-13.
- [19] O. Hajizad, A. Kumar, Z. Li et al. Influence of microstructure on mechanical properties of bainitic steels in railway applications, *Metals*, 9 (7), 778 (2019) 01-19.
- [20] A. Kumar, G. Agarwal, R. Petrov et al. Microstructural evolution of white and brown etching layers in pearlitic rail steels, *Acta Materialia*, 171 (2019) 48-64.
- [21] A. Kumar, S. K. Makineni, A. Dutta et al, Design of high-strength and damage-resistant carbide-free fine bainitic steels for railway crossing applications, *Materials Science and Engineering: A*, 759 (2019) 210-223.
- [22] T. Leitner, S. Sackl, B. Völker et al. Crack path identification in a nanostructured pearlitic steel using atom probe tomography, *Scripta Materialia*, 142 (2018) 66-69.
- [23] M. Zhu, G. Xu, M. Zhou et al, Effects of Tempering on the Microstructure and Properties of a High-Strength Bainite Rail Steel with Good Toughness. *Metals*, 8, 484 (2018) 01-11.
- [24] S. M. Hasan, D. Chakrabarti, S. B. Singh. Dry rolling/sliding wear behaviour of pearlitic rail and newly developed carbide-free bainitic rail steels. *Wear*, 408–409 (2018) 151–159.
- [25] W.T. Zhu, L.C. Guo, L.B. Shi et al. Wear and damage transitions of two kinds of wheel materials in the rolling-sliding contact, *Wear*, 398–399 (2018) 79–89.
- [26] X. J. Zhao, J. Guo, Q. Y. Liu. Effect of spherical dents on microstructure evolution and rolling contact fatigue of wheel/rail materials, *Tribology International*, 127 (2018) 520–532.
- [27] A. Ray. Niobium microalloying in rail steels, *Materials Science and Technology*, 33:14 (2017) 1584-1600.
- [28] D. Zeng, L. Lu, Y. Gong et al. Optimization of strength and toughness of railway wheel steel by alloy design, *Materials and Design*, 92 (2016) 998–1006.
- [29] L. B. Godefroid, L. P. Moreira, T. C. G. Vilela et al. Effect of chemical composition and microstructure on the fatigue crack growth resistance of pearlitic steels for railroad application, *International Journal of Fatigue*, 120 (2019) 241–25.

- [30] Q. Li, J. Guo, A. Zhao. Effect of upper bainite on wear behaviour of high-speed wheel steel. *Tribology Letters*, 67: 121 (2019) 01-09.
- [31] F. Fazeli, B. S. Amirkhiz, C. Scott et al. Kinetics and microstructural change of low-carbon bainite due to vanadium microalloying. *Materials Science & Engineering A*, 720 (2018) 248–256.
- [32] T. Sourmail, C. Garcia-Mateo, F. G. Caballero et al. The influence of vanadium on ferrite and bainite formation in a medium carbon steel. *Metallurgical and Materials Transactions A*, 48: (2017) 3985–3996.
- [33] C. Garcia-Mateo, L. Morales-Rivas, F. G. Caballero et al. Vanadium effect on a medium carbon forging steel. *Metals*, 6, 130 (2016) 01-12.
- [34] D. Zeng, L. Lu, Y. Gong et al. Influence of solid solution strengthening on spalling behavior of railway wheel steel. *Wear*, 372-373 (2017) 158–168.
- [35] P. P. Senthil, K. S. Raob, H. K. Nandia et al. Influence of niobium microalloying on the microstructure and mechanical properties of high carbon nano bainitic steel. *Procedia Structural Integrity*, 14 (2019) 729–737.
- [36] Y. Zhou, J. F. Peng, W. J. Wang, X. S. Jin, M. H. Zhu. Slippage effect on rolling contact wear and damage behavior of pearlitic steels. *Wear*, 362-363 (2016) 78–86.